PHYSICAL REVIEW B

CONDENSED MATTER

THIRD SERIES, VOLUME 48, NUMBER 23 15 DECEMBER 1993-I

Electronic structure and the metal-semiconductor transition in $BaPb_{1-x}Bi_xO_3$ studied by photoemission and x-ray-absorption spectroscopy

H. Namatame and A. Fujimori
Department of Physics, University of Tokyo, Bunkyo-ku, Tokyo 113, Japan

H. Takagi and S. Uchida
Department of Applied Physics, University of Tokyo, Bunkyo-ku, Tokyo 113, Japan

F. M. F. de Groot* and J. C. Fuggle†
Research Institute for Materials, University of Nijmegen, Toernooiveld, 6525 ED Nijmegen, The Netherlands
(Received 6 July 1993; revised manuscript received 30 August 1993)

We have studied the electronic structure of $BaPb_{1-x}Bi_xO_3$ and its changes across the composition-dependent metal-semiconductor transition using photoemission and O 1*s* x-ray-absorption spectroscopy. For the parent insulator $BaBiO_3$, the peak-to-peak splitting of the Bi 6*s* band is found to be large, whereas, the minimum gap is much smaller, qualitatively consistent with the large ($\sim$2 eV) optical gap of the direct type and the smaller ($\sim$0.5 eV) transport gap of indirect type. Pb substitution for Bi induces new states of Pb 6*s* character *outside* the band gap of $BaBiO_3$ and does not induce in-gap spectral weight unlike in cuprate superconductors; the splitting of the Bi 6*s* band is not significantly reduced by Pb substitution throughout the semiconducting region. Substituted Pb remains tetravalent in the semiconducting phase and does not supply the Bi-O network with extra holes, which explains the stability of the semiconducting phase up to the Pb content of $\sim$65%. Nevertheless, the band gap collapses in the metallic region ($x<0.35$), where a clear Fermi edge is observed. The shifts of the core-level and valence-band peaks with x suggest that a small ($\sim$0.3 eV) rigid-band shift of the Fermi level occurs in the metallic region. Comparison of the photoemission, optical absorption, and transport data on $BaBiO_3$ strongly suggests that polaronic levels are created within the band gap of $BaBiO_3$ and accommodate thermally excited charge carriers.

I. INTRODUCTION

Recently, $BaPb_{1-x}Bi_xO_3$ has attracted revived interest following the discovery of high-temperature superconductivity in $Ba_{1-x}K_xBiO_3$.[1] Both have superconducting transition temperatures (T_C) of the same order of magnitude as those of $A15$-type superconductors, in spite of the density of states (DOS) one order of magnitude lower at the Fermi level (E_F):[2] $Ba_{1-x}K_xBiO_3$ (BKBO) shows the highest T_C of 30 K at $x\approx0.4$,[1] which is comparable to the T_C of $La_{2-x}Sr_xCuO_4$. $BaPb_{1-x}Bi_xO_3$ (BPBO) shows a metal-semiconductor transition as a function of composition; it shows superconductivity in the metallic region, $0<x<0.35$,[3-5] where the highest T_C of 12 K occurs at $x\approx0.25$. The parent insulator of BPBO and BKBO, $BaBiO_3$, does not contain magnetic ions, excluding pairing mechanisms mediated by magnetic fluctuations. The crystal structures of BPBO and BKBO are of the cubic (or distorted) perovskite type, unlike the layered-type cuprate superconductors.

Since the average Bi valence in $BaBiO_3$ is 4+, a cubic $BaBiO_3$, if it existed, would be a metal with a half-filled Bi 6*s* conduction band. Actually, $BaBiO_3$ has a frozen breathing-type displacement of oxygen atoms around the Bi atoms combined with the tilting of the BiO_6 octahedra,[6,7] which is thought to be responsible for the semiconducting band gap of $BaBiO_3$. This structure can be viewed as a charge disproportionation of Bi atoms into Bi^{3+} and Bi^{5+}, or the formation of a charge-density wave (CDW) at the Bi sites. The CDW is thought to be quite "local," having a very short coherence length of the order of the lattice parameters as estimated from the large optical gap of $\sim$2 eV.[8] Previous band-structure calculations have not been successful in predicting the insulating band gap of $BaBiO_3$ in the cubic structure or in the breathing-type distorted structure.[9,10] However, a recent

band-structure calculation[11] has shown an opening of the band gap when the tilting and the breathing of the BiO_6 octahedra are simultaneously taken into account. Nevertheless, it remains an open question why the semiconducting phase of BPBO is stable for such a large amount of Pb substitution ($\sim 65\%$), whereas the semiconducting phase of BKBO is destroyed by the relatively small amount of K substitution ($\sim 35\%$). In order to answer this question, the microscopic nature of the composition-dependent metal-semiconductor transition has to be clarified. Also, the anomalous semiconducting behavior of $BaBiO_3$ has led to the suggestion of the formation of extremely narrow Bi 6*s* bands and an associated semiconducting mechanism.[8]

$BaPbO_3$ is a semimetal according to the band-structure calculations.[9,10] Indeed, upon Bi substitution for Pb, carrier concentration deduced from Hall effect and plasma edges linearly increases with x until $x \sim 0.17$,[4,5] where each substituted Bi atom is thought to donate one electron to the Pb 6*s*-derived conduction band of $BaPbO_3$. For low Bi concentration ($x < 0.17$), the optical conductivity spectra can be well fitted to the Drude model, whereas for higher Bi concentration the spectra gradually deviate from the Drude curve; above $x \approx 0.17$ the optical conductivity spectra consist of the sum of free-carrier absorption and interband transition.[4,5] Tajima *et al.*[4,5] considered that the interband transition occurs between the Bi 6*s* bands which are split due to a local or dynamical charge disproportionation at the Bi sites and form a pseudogap even in the metallic phase. The optical band gap of $BaBiO_3$ is 1.9 eV[4,5] whereas the activation energy deduced from transport measurements is as small as 0.24 eV.[8]

So far, several photoemission studies have been reported on BPBO,[12–15] but no evidence for the charge disproportionation has been found. Matsuyama *et al.*[13] have measured ultraviolet photoemission (UPS) spectra and found that in going from $BaBiO_3$ to $BaPb_{0.85}Bi_{0.15}O_3$, the O 2*p* peak in the valence band is shifted toward lower binding energy by ~ 0.3 eV, implying a small rigid-band shift caused by the substitution. Empty states in BPBO have been studied by O 1*s* x-ray-absorption spectroscopy (XAS) (Ref. 16) and inverse-photoemission spectroscopy.[17] In the present paper, we have made detailed studies of the electronic structure of BPBO by using UPS and x-ray-photoemission spectroscopy (XPS) combined with the XAS data with particular emphasis on substitution-induced changes in the electronic states near the Fermi level across the metal-semiconductor transition. In addition, detailed analysis of the spectra has yielded interesting information on the polaronic states in the semiconducting $BaBiO_3$.

II. EXPERIMENT

Single crystals were prepared by the flux method using a solvent of PbO_2 and Bi_2O_3. The compositions of the single crystals we studied were $x = 0$, 0.25, 0.4, 0.7, and 1.0.

UPS measurements were performed using the He I ($h\nu = 21.2$ eV) and He II ($h\nu = 40.8$ eV) resonance lines, and XPS measurements using the Mg K_α line ($h\nu = 1253.6$ eV). Photoelectrons were collected using a double-pass cylindrical-mirror analyzer. The total-energy resolution was ~ 0.2 eV for UPS, and ~ 1 eV for XPS. The samples were glued to copper plates with conductive epoxy (Epotek E20C) and their surfaces were scraped *in situ* with a diamond file. Scraping was repeated until O 1*s* XPS spectra became a single peak [see Fig. 1(a)]. Scraping and measurements were repeated at liquid-nitrogen temperature (LNT) to prevent surface degradation under the ultrahigh vacuum of $\sim 2 \times 10^{-10}$

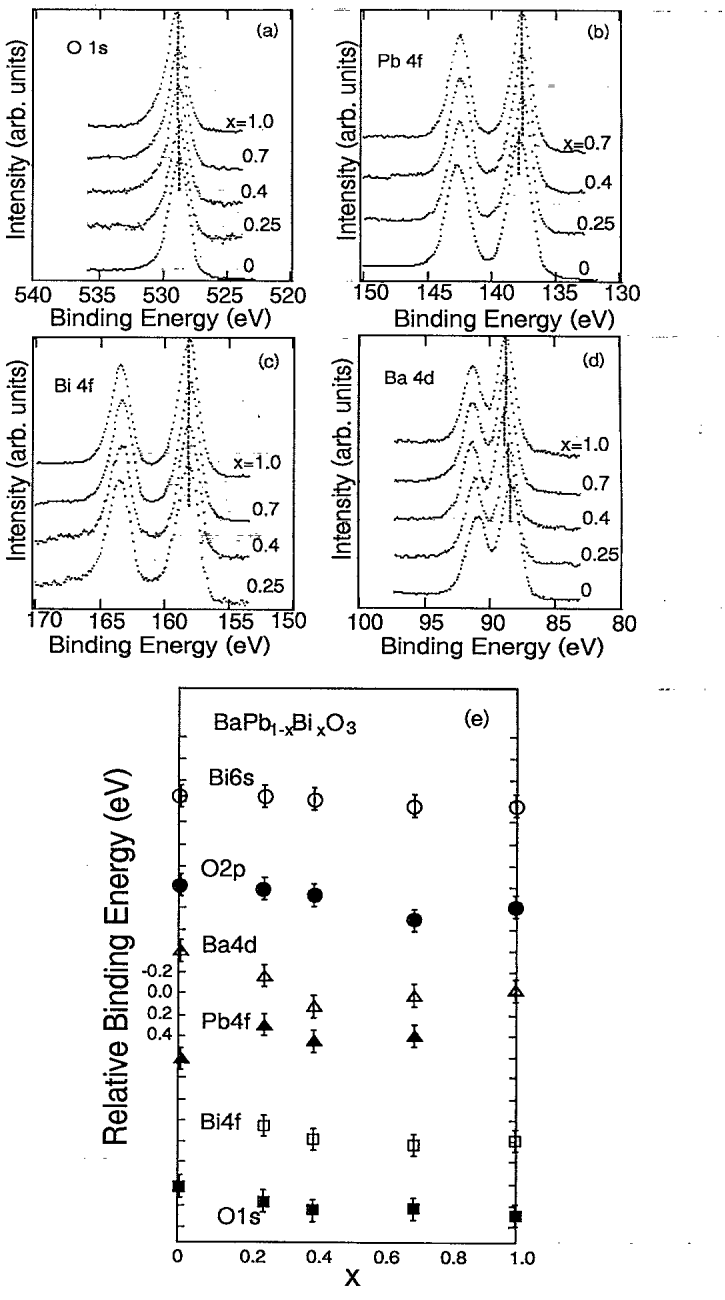

FIG. 1. XPS spectra of the O 1*s* (a), Pb 4*f* (b), Bi 4*f* (c), and Ba 4*d* (d) core levels in $BaPb_{1-x}Bi_xO_3$. The vertical lines mark the peak positions. (e) Relative core-level and valence-band peak positions as functions of x.

Torr. When a surface degradation occurred, additional structures appeared on the high-binding-energy side of the O 1*s* peak as a shoulder. The additional structure grew slowly with time and could be again diminished by scraping. At LNT, the O 1*s* line shape stays "clean" for ~40 min after scraping. In the UPS spectra, a structure originating from surface degradation appeared around 9 eV below E_F and grew within ~30 min at LNT, as in high-T_C superconductors. $BaBiO_3$ showed appreciable charging effects at LNT. Therefore, measurements were repeated at room temperature with more frequent scraping for $BaBiO_3$ as well as for the other compositions. A $BaPbO_3$ sample was cooled down to ~35 K using a closed-cycle He refrigerator, cleaved and measured at beamline BL-11D of Photon Factory, National Laboratory for High Energy Physics (KEK-PF). The spectra at ~35 K, LNT, and room temperature thus measured were almost identical to each other except for the charging effects in $BaBiO_3$ at LNT, ensuring that the spectra presented here are those of intrinsic samples and not of degraded or contaminated surfaces. Au was evaporated on the surface of every sample to determine the Fermi-level position in UPS and the binding energies of the XPS spectra.

O 1*s* XAS measurements were performed on polycrystalline samples (supplied by J. M. van Ruitenbeek) at Berliner Elektronenspeicherung Geselleschaft für Synchrotronstrahlung (BESSY) by using a SX700(I) plane-grating monochromator. The instrumental resolution was ~0.5 eV FWHM (full width at half maximum), and the O 1*s* core-hole lifetime broadening was 0.3 eV. Details of the XAS measurements are described in Ref. 16.

III. RESULTS AND DISCUSSIONS

A. Composition-dependent energy shifts

Figures 1(a)–1(d) show the XPS spectra of the O 1*s*, Pb 4*f*, Bi 4*f*, and Ba 4*d* core levels. The sharp O 1*s* peaks without high-binding-energy components demonstrate the cleanliness of the sample surfaces. The Bi 4*f* spectra show a simple spin-orbit doublet structure.[15] The Bi 4*f* spectrum of $BaBiO_3$ does not show two components corresponding to Bi^{3+} and Bi^{5+} as in previous studies. Instead, each peak was successfully fitted by a single Lorentzian convoluted with a Gaussian of the same width as those used for the other core levels, indicating that the Bi^{3+}-Bi^{5+} splitting, if existed, should be very small. Figure 1(e) shows that with increasing Pb concentration the O 1*s*, Ba 4*d*, and Bi 4*f* core-level peaks are all shifted toward lower binding energies (by ~0.3 eV in going from $BaBiO_3$ to $BaPbO_3$), although there are subtle differences in the shifting behavior between the different core levels. The Pb 4*f* peak, on the other hand, exhibits a complicated shift, particularly for small *x*'s.

Figure 2 shows UPS spectra in the valence-band region. As in the O 1*s* and Ba 4*d* core levels, the prominent peak at ~3 eV below E_F is also shifted toward lower binding energy by ~0.3 eV in going from $BaBiO_3$ to $BaPbO_3$. The binding energies of the core-level and valence-band peaks except for Pb 4*f* commonly decreases

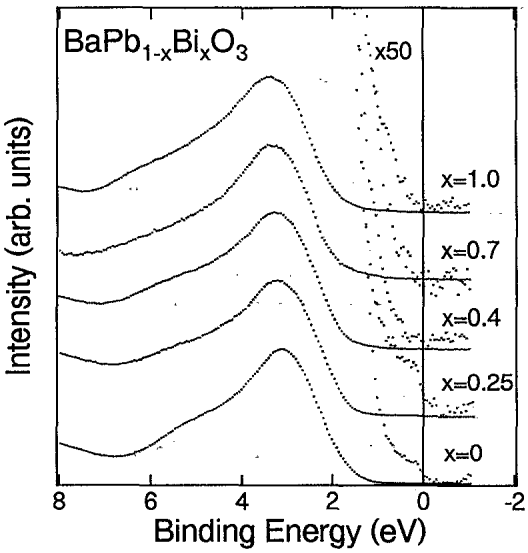

FIG. 2. UPS spectra of $BaPb_{1-x}Bi_xO_3$ taken with $h\nu=40.8$ eV. The peak position of the O 2*p* band is marked by vertical lines. A magnified view around E_F is given for each spectrum.

with Pb concentration [Fig. 1(e)], implying a downward shift of the chemical potential or E_F with Pb substitution. The non-rigid-band behavior of the Pb 4*f* core level for small *x*'s may be due to the screening of the Pb core hole by electrons occupying the bottom of the Pb 6*s* band, as we shall discuss below. If we consider that the Ba 4*d* core-level shift most faithfully reflects the chemical potential shift (since electronic states associated with Ba are not involved in chemical bonding nor in the metallic conductivity), we may conclude that the significant chemical potential shift occurs mainly in the metallic region[18] and not in the semiconducting region. In any case, the amount of the shift, ~0.3 eV, is much smaller than that ($\lesssim$2 eV) predicted by the band-structure calculations,[9,10] implying that electrons in BPBO cannot naively be described as conventional, noninteracting Bloch electrons.

B. Gross electronic structure of the end members

In Fig. 3, the valence-band UPS spectra and the O 1*s* XAS spectra[16] are compared with the theoretical spectra calculated using the O 2*p* and Bi/P 6*s* partial DOS given by Takegahara and Kasuya[10] multiplied by the atomic subshell photoionization cross sections.[19] The calculation on $BaBiO_3$ (with the hypothetical cubic structure) shows that Bi 6*s* and O 2*p* states hybridize to form Bi 6*s*–O 2*p* bonding states ~10 eV below E_F and its counterpart, half-filled antibonding states around E_F; O 2*p* nonbonding states are calculated to be between them, namely 2–6 eV below E_F. $BaPbO_3$ has Pb 6*s*–O 2*p* bonding and antibonding states around ~7 eV below E_F and ~2 eV above E_F, respectively, and O 2*p* nonbonding states 0–4 eV below E_F. That is, a rigid-band shift of ~2 eV has been predicted by the band-structure calculation. Now the prominent peak observed around 3 eV is unambiguously assigned to the O 2*p* nonbonding states. The Bi 6*s*–O 2*p* antibonding states in $BaBiO_3$ are observed just below E_F in agreement with the calculation, al-

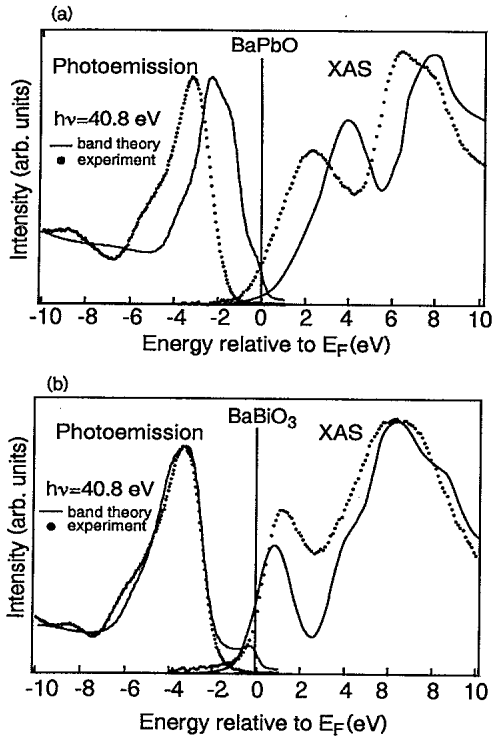

FIG. 3. Comparison of the UPS and O 1*s* XAS spectra with band theory for $BaPbO_3$ (a) and $BaBiO_3$ (b). The dotted curves show the measured spectra, and the solid curves show spectra calculated using the DOS given by band-structure calculations (Ref. 10). For the UPS spectra, the O 2*p* and Bi/Pb 6*s* partial DOS have been multiplied by the corresponding cross sections. For the XAS spectra, the O 2*p* partial DOS is used. The calculated DOS has been broadened with Lorentzian and Gaussian functions to simulate the instrument and lifetime broadening.

though the observed intensity is much smaller than the calculation, as we shall discuss below. The Bi 6*s*–O 2*p* bonding states have been identified ~6 eV below E_F in our previous valence-band XPS study,[20] considerably shallower than predicted by the calculation.

The empty states hybridizing with O 2*p* states are studied by O 1*s* XAS spectroscopy. In order to define the Fermi-level position in the XAS spectra, the O 1*s* XPS binding energies were tentatively used as the threshold energies of the O 1*s* absorption.[21] The first peak in the unoccupied part of the calculated DOS is due to the Pb 6*s*–O 2*p* or Bi 6*s*–O 2*p* antibonding states (hereafter referred to as Pb 6*s* and Bi 6*s* states for simplicity). Therefore, in the XAS spectra, the peak ~1 eV above E_F in $BaBiO_3$ is assigned to the empty Bi 6*s* states, and the peak at ~2.2 eV in $BaPbO_3$ to the empty Pb 6*s* states, each hybridizing with O 2*p* states.[16]

In the calculated photoemission spectrum of $BaBiO_3$, the Bi 6*s* band located around E_F shows a high intensity, whereas the experimental spectrum shows a much lower intensity in that energy region. Because of the negligibly small Bi 6*s*–O 2*p* relative cross sections ($\sim 4\times10^{-2}$) for $h\nu\sim40$ eV,[19] the discrepancy between the calculated and experimental spectra is attributed to an overestimate of the Bi 6*s*–O 2*p* hybridization in the band-structure calculation. This is probably due to the cubic crystal structure assumed in the calculation: The Bi-O distance around the "Bi^{3+}" site whose electronic states constitute the occupied part of the Bi 6*s* band is larger than the average Bi-O distance and therefore the occupied Bi 6*s* band would actually be much more weakly hybridized with the O 2*p* states. Indeed, in the XPS spectra, where the Bi 6*s*–O 2*p* relative cross section is much larger (~7), the Bi 6*s* emission near E_F has been identified with high intensity.[20] The O 2*p* nonbonding states corresponding to the observed peak at ~3.4 eV are in good agreement with the calculation.

As for $BaPbO_3$, there is a more pronounced discrepancy between the experimental and calculated spectra in that the calculated spectrum predicts a high DOS just below E_F and an O 2*p* main peak position as shallow as 2 eV, whereas the experimental spectrum shows a very low intensity around E_F and the O 2*p* peak is located at ~3.1 eV. The Pb 6*s*–O 2*p* antibonding states are calculated to be ~4 eV above E_F, although the experimental one is located around ~2.6 eV above E_F. Here we would like to emphasize again that the measurement for $BaPbO_3$ was performed on a single crystal *in situ* cleaved at ~35 K and therefore we believe that the spectral features are intrinsic. It is surprising that the discrepancy between the calculation and experiment is more pronounced for $BaPbO_3$ than for $BaBiO_3$,[22] considering the fact that the cubic crystal structure for $BaPbO_3$ assumed in the calculation is close to the real crystal structure. Possible origins of the discrepancy will be discussed in Sec. III E.

C. Evolution of electronic states near the Fermi level with chemical composition

In the UPS spectra (Fig. 2) one can observe weak but clear Fermi edges for the metallic compositions ($x=0$ and 0.25); the height of the Fermi edge becomes the largest for $x=0.25$. This is consistent with the transport measurements,[3] which show that the metallic carrier density as well as T_C increases with Bi substitution from $x=0$, until $x\approx0.25$, and then decreases toward the metal-semiconductor phase boundary at $x\approx0.35$. The He I UPS spectra showed stronger emission at E_F, as reported by Matsuyama *et al.*,[13] but detailed analysis was hindered by overlapping Pb 5*d* core-level peaks excited by the He II radiation.

In order to highlight the changes in the spectra near E_F caused by the Bi substitution, we have plotted in Fig. 4 the difference spectra of BPBO from that of $BaPbO_3$. Prior to subtraction, the O 2*p* main peak was aligned as shown in Fig. 4(a). The difference spectra can then be regarded as a contribution from the Bi 6*s* (–O 2*p* antibonding) states under the assumption that the valence band of $BaPbO_3$ is mainly composed of nonbonding O 2*p* states and that the O 2*p* valence band DOS does not change much with Bi substitution. Figure 4 shows that with increasing Bi concentration x, the Bi 6*s* emission intensity increases around E_F. The difference spectra for $x=0.25$ shows a trapezoid shape which decreases in intensity toward E_F. At this Bi concentration, local distortion has been found around the Bi atoms,[7] so that the intensity

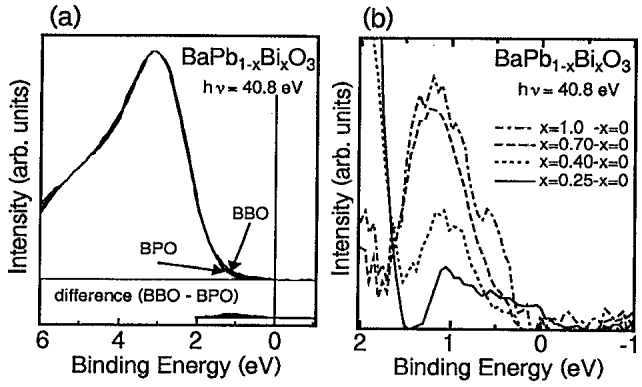

FIG. 4. Difference UPS spectra ($h\nu$=40.8 eV) between $BaPb_{1-x}Bi_xO_3$ and $BaPbO_3$ around E_F, which highlight the Bi 6*s* contribution. (a) Spectra of $BaPbO_3$ and $BaBiO_3$, whose O 2*p* valence peaks are aligned and which are subtracted from one another to obtain the difference spectrum. (b) Difference spectra for $BaPb_{1-x}Bi_xO_3$ near E_F.

decrease toward E_F may be related to the DOS of the Bi 6*s* band which forms a shallow pseudogap in the metallic state. In going from the metallic to the semiconducting regions ($x > 0.35$), the peak in the difference spectra is a little shifted toward higher binding energy [Figs. 1(e) and 5], corresponding to the opening of the energy gap. If we assume that the integrated area of the difference spectrum within ~2 eV of E_F is proportional to x, i.e., the number of electrons in the Bi 6*s* band, then the DOS at E_F can be estimated from the height of the Fermi edge to be ~0.1 states/eV unit formula. This value is in reasonable agreement with that derived from the electronic specific heat (0.14 states/eV unit formula) and that obtained by the band-structure calculations (0.13 states/eV unit formula). This implies that the ordinary

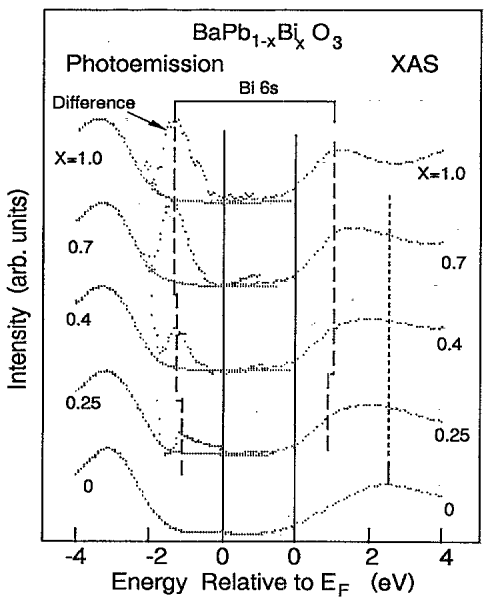

FIG. 5. Combined UPS and O 1*s* XAS spectra of $BaPb_{1-x}Bi_xO_3$. The difference UPS spectra are the same as those shown in Fig. 4(b).

band picture is applicable to the electronic states in the vicinity of E_F of the metallic state, in spite of the existence of the pseudogap feature and the inapplicability of the rigid-band model.

Alternatively, we may start from $BaBiO_3$ and consider the evolution of electronic states caused by Pb substitution. The Bi 6*s* emission decreases in intensity [Figs. 1(b) and 5] but its position does not shift significantly even though the band gap eventually collapses in the metallic phase ($x < 0.35$).

Figure 5 shows the combined UPS and O 1*s* XAS spectra of $BaPb_{1-x}Bi_xO_3$ for various x's. The widths of the occupied and unoccupied Bi 6*s* bands are both $\gtrsim 1$ eV, whereas the unoccupied Pb 6*s* bandwidth is twice as large as those of the Bi 6*s* bands. For the intermediate Bi concentrations, the overlapping Bi 6*s* and Pb 6*s* bands in the XAS spectra leads to an even broader peak with weak structures identified at ~1 and ~2.6 eV. The latter structures correspond well to the unoccupied Bi 6*s* and Pb 6*s* bands in $BaBiO_3$ and $BaPbO_3$ located, respectively, at ~1 and ~2.6 eV above E_F. Indeed, we have successfully fitted the XAS spectra of the intermediate compositions (except for $x = 0.25$) by a superposition of the spectra of $BaPbO_3$ and $BaBiO_3$ with the corresponding Pb-to-Bi atomic ratios, indicating that Pb substitution for Bi in $BaBiO_3$ induces empty states of Pb 6*s* character well above E_F. Since Pb has one less electron than Bi, the empty Pb 6*s* states mean that the substituted Pb remains tetravalent at least in the semiconducting region, and that Pb substitution does not supply the Bi-O network with extra holes as has been widely believed. Indeed, upon Pb substitution the Fermi level *does not* move to the top of the lower Bi 6*s* band as would be expected from the rigid-band model of hole doping. Only the XAS spectrum of $x = 0.25$ could not be reproduced by the same superposition, but is shifted as a whole toward lower energies by ~0.8 eV. This suggests that the unoccupied Bi 6*s* states are located closer to E_F in the metallic composition than in the semiconducting compositions, although detailed analysis of the line shapes of the O 1*s* XAS spectra are difficult because of the core-hole lifetime broadening and possible effects of the core-hole potential. The evolution of the electronic structure thus deduced are schematically illustrated in Fig. 6. As implied by Fig. 5, although the band gap collapses in the metallic phase, there is no clear indication of a complete collapse of the Bi 6*s* bands into a single band, suggesting the formation of a pseudogap in the metallic phase.

D. Nature of the band gap and the semiconducting properties of $BaBiO_3$

The semiconducting properties of $BaBiO_3$ are derived from the splitting of the Bi 6*s* band which arises from the complicated lattice distortion. Recently, Liechtenstein *et al.*[11] have searched for the lowest total energy of $BaBiO_3$ by incorporating both the breathing-type distortion around the Bi atoms and the tilting of the BiO_6 octahedra. They have found that the Bi 6*s* band is split to form a finite (~0.3-eV) indirect band gap when an appropriate combination of the two types of lattice distor-

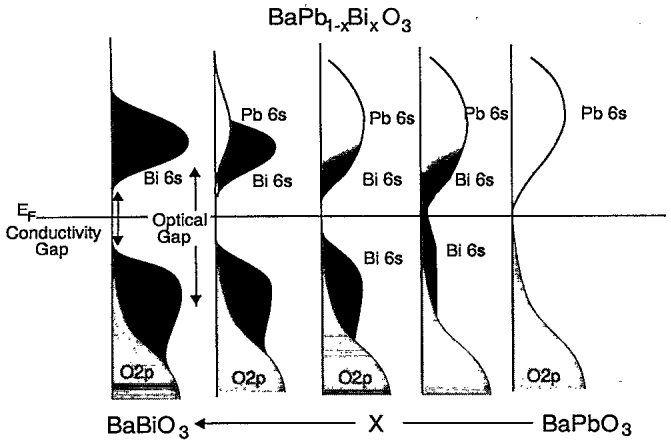

FIG. 6. Schematic representation of the electronic structure of $BaPb_{1-x}Bi_xO_3$. The energies are referenced to the chemical potential (E_F), which moves downward by ~0.3 eV in going from $BaBiO_3$ to $BaPbO_3$. For a detailed description, see text.

tions is considered. With this structure, the charge difference within the Bi muffin-tin spheres is found to be less than 0.1 electrons, consistent with the absence of detectable Bi^{3+}-Bi^{5+} splitting in the Bi core-level photoemission spectra.

Experimentally, the optical band gap of $BaBiO_3$ has been found to be 1.9 eV,[4,5] whereas the activation energy of electrical conductivity above ~200 K is only 0.24 eV.[5,8] From the photoemission and XAS spectra of $BaBiO_3$, the peak-to-peak splitting between the occupied and unoccupied Bi 6*s* states is found to be 2.1 eV, which is incidentally close to the optical band gap of $BaBiO_3$. On the other hand, finite photoemission intensity in $BaBiO_3$ starts from ~0.4±0.05 eV below E_F (Fig. 2), which is on the same order as the activation energy. These findings can be understood in terms of Liechtenstein *et al.*'s band structure, where the split Bi 6*s* bands form a direct gap of ~1.3 eV, and the indirect one of ~0.3 eV, considering the fact that band gaps are generally underestimated (by ~0.6 eV in this case, see below) in band-structure calculations using the local-density approximation (LDA). However, according to the Hall effect measurement by Takagi *et al.*[8] at $T \gtrsim 200$ K the number of states which contribute to the electrical conductivity is comparable to the number of Bi atoms, meaning that the 0.24-eV activation energy corresponds to the intrinsic band gap (i.e., it is not due to impurities), and that the Bi 6*s* bandwidths are on the order of kT. In order to reconcile the large Bi 6*s* bandwidths (~1 eV) observed by photoemission, XAS, and the band-structure calculation with the narrow ones (~kT) deduced from the transport properties, we propose that the thermally excited charge carriers in semiconducting $BaBiO_3$ are polarons with substantial band narrowing due to the strong electron-phonon coupling. The large optical band gap is then attributed to a Franck-Condon transition in which the lattice is frozen, and which reflects the joint DOS of the frozen lattice given by the band-structure calculations. Photoemission and XAS are also Frank-Condon-type "fast" probes and therefore yield the DOS of the frozen lattice.

In the intrinsic conduction region ($\gtrsim 200$ K), the number of thermally excited electrons and that of holes must be the same, and the Fermi level must be located in the midpoint of the transport gap. The positive Hall coefficient[8] indicates that the mobile charge carriers are holes created in the occupied Bi 6*s* band, and that electrons are not sufficiently mobile to contribute to the electrical conductivity. The 0.24-eV activation energy therefore gives the position of the polaronic hole band states relative to E_F. Thus, as shown in Fig. 7, the polaronic band states lie between the E_F and the top of the occupied Bi 6*s* band of the frozen lattice located ~0.4 eV below E_F but cannot be reached by photoemission. That is, the polaronic band is located ~0.15 eV (=~0.4–0.24 eV) above the occupied Bi 6*s* band of the frozen lattice, meaning that the binding energy of the hole polaron is ~0.15 eV. If we assume that the underestimation of the direct band gap in the LDA band structure of $BaBiO_3$ (by ~0.6 eV) is *uniform* throughout the Brillouin zone,[23] then the indirect gap of the frozen lattice is estimated to be ~0.9 eV (=0.3+0.6 eV). In the intrinsic semiconduction region, the polaronic states of the electron carriers must be located 0.24 eV above E_F or ~0.25 eV (≃0.9–0.4–0.24 eV) below the bottom of the empty Bi 6*s* band, as can be seen in Fig. 7. The polaron binding energy of the electron is larger than that of the hole, consistent with the low mobility of the electrons. So far, the polaronic nature of the charge carriers in $BaBiO_3$ has been demonstrated by photoinduced changes in the optical-absorption spectra.[24] Photoinduced absorption at $h\nu \approx 0.9$ eV (Ref. 25) may be interpreted as due to the indirect optical transition which became allowed by the broken symmetry around the photoinduced polaronic carriers. Here, we emphasize that a simple semiconductor picture with an indirect band gap of ~0.5 eV, which leads to the activation energy of ~0.25 eV and is compatible with the photoemission data if a band bending near the surface is assumed, cannot be reconciled with the transport properties which show the valence-band width of order ~kT, orders of magnitude

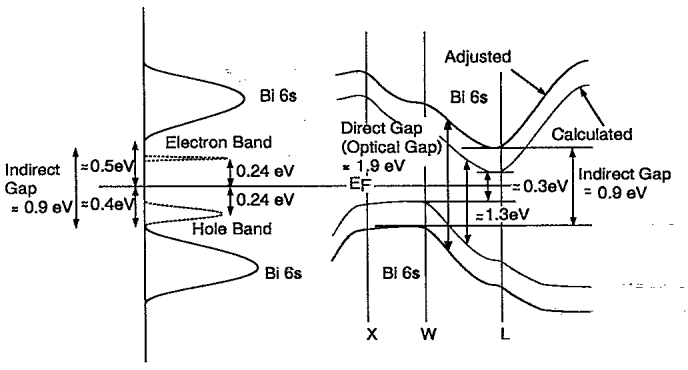

FIG. 7. Proposed electronic structure of $BaBiO_3$ in the vicinity of the Fermi level. Left: DOS of the frozen lattice (solid lines) and polaronic states (dashed lines) formed within the band gap of the frozen lattice. Right: Band dispersion in the Brillouin zone. Calculated dispersion (Ref. 11) has been adjusted to yield the 1.9-eV optical band gap as shown in the figure.

narrower than the calculated width of the occupied Bi 6*s* band.

It is interesting to note that in cuprate superconductors, the difference in the Fermi-level position between *p*-type $La_{2-x}Sr_xCuO_4$ and *n*-type $Nd_{2-x}Ce_xCuO_4$ as measured by photoemission is only a small fraction (~ 0.3 eV) of the optical band gap (1.5–2.0 eV).[25] As the band gaps of the parent insulators are most probably of the direct type,[26] the small Fermi-level difference means that the Fermi level must be pinned well inside the band gaps. [The binding energy of charge carriers to the impurity potential must be very small ($\ll 0.1$ eV),[27] and can be neglected.] If the polaronic in-gap levels are formed within the band gaps of the parent compounds as in $BaBiO_3$, then upon electron and hole doping the Fermi level would move to the electron- and hole-accommodating polaronic levels, respectively, resulting in a Fermi-level difference which is smaller than the optical band gaps. Analysis of experimental data along this line would give interesting insights into the electronic structure of the cuprate superconductors.

E. Semimetallic $BaPbO_3$

The band-structure calculations have shown that $BaPbO_3$ is a semimetal with a finite overlap between the Pb 6*s* and O 2*p* bands around E_F.[9,10] Since the band-structure calculations on $BaPbO_3$ have been done on a cubic structure which is close to the real orthorhombic one, it is difficult to explain the discrepancy between the experimental and calculated spectra, namely the observed low photoemission intensity within ~ 1 eV of E_F and the calculated high DOS in this region. De Groot, Fuggle, and van Ruitenbeek[16] examined the effect of oxygen defects in the XAS spectra by studying variously treated samples, but they could not find any changes in their spectra excluding the possibility that the discrepancy is due to oxygen off-stoichiometry. As the origin of the discrepancy between the calculation and experiment, we may consider the following possibilities.

(i) $BaPbO_3$ is actually a wide-gap insulator with a band gap of ~ 1 eV like $BaSnO_3$,[28] which is isoelectronic to $BaPbO_3$. The actual $BaPbO_3$ sample, which is an *n*-type metal, should have a sufficient amount of oxygen vacancies and be doped with extra electrons. However, from a recent optical study of reduced $BaPbO_3$ samples, it has been suggested that the stoichiometric $BaPbO_3$ already has a finite number of electron carriers.[29]

(ii) Electron-electron interaction among the carriers may distort the spectra from the DOS given by the LDA band-structure calculation. In order to test this possibility, we have calculated the DOS of an electron gas using the Hartree-Fock approximation,[30] i.e., without resorting to the LDA for the exchange potential. The carrier density and the effective mass of the electron gas have been taken equal to those of $BaPbO_3$. Thus we find that the DOS within ~ 0.5 eV of E_F is reduced by $\sim 10\%$ due to the nonlocal effect of the Coulomb-exchange interaction (screened beyond the Thomas-Fermi length). This effect is still too weak to explain the observed low photoemission intensity within ~ 1 eV of E_F.

(iii) Charge carriers in $BaPbO_3$ are strongly polaronic. The energy gap between the polaronic electron (Pb 6*s*) and hole (O 2*p*) bands is closed while that of the frozen lattice is not closed. Then the photoemission intensity can be very low around E_F. In this picture, the hole polaron binding energy has to be as large as ~ 1 eV, implying a very heavy mass for the hole carriers, whereas the electron polaron binding energy must be small because the *n*-type metallic carriers have a light effective mass ($m^*/m \sim 0.5$).[4]

At present, none of the above mechanisms seem satisfactory to explain the photoemission spectra. A combination of the above mechanisms and/or others may be responsible for the experimental observation. In order to clarify this point, further studies are necessary.

IV. SUMMARY AND CONCLUDING REMARKS

In this paper, we have reported the photoemission and O 1*s* XAS spectra of $BaPb_{1-x}Bi_xO_3$ with varying Bi concentrations. The Pb substitution does not supply the Bi-O network with extra holes because the valence of Pb remains 4+ in the semiconducting state: The empty Pb 6*s* states are located well above E_F, and simply replace the half-filled Bi 6*s* states. No spectral weight is induced within the band gap in the semiconducting phase in contrast to the case of carrier-doped Cu oxides, where so-called in-gap *spectral weight* develops with carrier doping. The stability of the semiconducting phase in the wide Pb concentration range is thus naturally understood.

If we view the system from the semimetallic $BaPbO_3$ side, a different picture emerges. Upon Bi substitution, Bi-derived states appear around E_F and hybridize with the bottom of the Pb 6*s* conduction band. Electrons supplied by the Bi atoms populate the Bi-Pb 6*s* band as if the bottom of the Pb 6*s* band is occupied by the electrons donated by Bi. This band filling is reflected upon the upward shift of the chemical potential, as suggested by the core-level shifts. With increasing x, the conduction band splits and shows a pseudogap behavior probably due to the local structural fluctuation, while the DOS at E_F reaches a maximum around $x \sim 0.25$ where the T_C becomes highest. The real gap is almost fully developed for $x > 0.35$, where the semiconducting state is realized.

$BaBiO_3$ is a semiconductor where the split Bi 6*s* bands form a direct gap of 1.9 eV and a smaller (~ 0.9-eV) indirect gap. From the photoemission spectra combined with the optical and transport data,[8] we propose that a hole-accommodating polaron band is formed above the top of the occupied Bi 6*s* band, and an electron-accommodating polaron band below the bottom of the empty Bi 6*s* band. These polaronic in-gap levels result in the reduction of the conductivity gap from ~ 0.9 eV of the frozen lattice to ~ 0.5 eV, yielding the 0.24-eV activation energy of the intrinsic semiconductivity.

So far, many theoretical works[32–37] have attempted to interpret the metal-semiconductor transition and superconductivity in BPBO. These studies differ in the way they assumed the energy difference between the Bi and Pb sites, and modeled the electron-phonon interaction.

Sofo, Aligia, and Regueiro[34] have proposed a model which takes into account the energy difference between the Bi 6*s* and Pb 6*s* levels, and the coupling between the local breathing-type lattice distortion and the electrons at the Bi sites, although the breathing mode is always frozen for any Bi concentration. This model qualitatively reproduces the observed spectral changes with substitution, in that the pseudogap appears already in the metallic region. Inada and Ishii[36] have assumed that the metal-semiconductor transition occurs when the gap between the bottom of the Pb 6*s* band and the occupied Bi 6*s* band is closed. Then, in order to reproduce the metallic behavior for small x, where electrons apparently occupy the bottom of the Pb 6*s* band, the Pb site energy cannot be significantly higher than the Bi site energy. Such a level ordering differs from our interpretation of the O 1*s* XAS spectra.

In conclusion, we have obtained a reasonable picture of the electronic structure of $BaPb_{1-x}Bi_xO_3$ ranging from the semiconducting to the superconducting regimes. However, there still remain several unresolved problems such as the interpretation of the $BaPbO_3$ data. Also, the polaronic interpretation of the spectra of $BaBiO_3$ is still tentative, and must be confirmed by further studies on this and related materials. More detailed information about the changes in the electronic structure in the vicinity of the composition-dependent metal-semiconductor transition is also an interesting problem to be pursued in future studies.

ACKNOWLEDGMENTS

We would like to thank Dr. H. Eisaki for collaboration and many useful discussions. This work is supported by a Grant-in-Aid for Scientific Research from the Ministry of Education, Science and Culture, Japan. The work at KEK-PF has been performed under the approval of the Photon Factory Program Advisory Committee (Proposal No. 91-241).

*Present address: LURE, Batiment 209D, 91405 Orsay, France.
†Deceased.

[1]R. J. Cava, B. Batlogg, J. J. Krajewski, R. Farrow, L. W. Rupp, Jr., A. E. White, K. Short, W. F. Peck, and T. Kometani, Nature **332**, 814 (1988).

[2]T. Itoh, K. Kitazawa, and S. Tanaka, J. Phys. Soc. Jpn. **53**, 2668 (1984).

[3]T. D. Thanh, A. Koma, and S. Tanaka, Appl. Phys. **22**, 205 (1980).

[4]S. Tajima, S. Uchida, A. Masaki, H. Takagi, K. Kitazawa, S. Tanaka, and A. Katsui, Phys. Rev. B **32**, 6302 (1985).

[5]S. Tajima, S. Uchida, A. Masaki, H. Takagi, K. Kitazawa, S. Tanaka, and S. Sugai, Phys. Rev. B **35**, 696 (1987).

[6]C. Chaillout, A. Santoro, J. P. Remeika, A. S. Cooper, G. P. Espinosa, and M. Marezio, Solid State Commun. **65**, 1363 (1988).

[7]J. B. Boyce, F. G. Bridges, T. Claeson, T. H. Geballe, G. G. Li, and A. W. Sleight, Phys. Rev. B **44**, 6961 (1991); A. Balzarotti, A. P. Menushenkov, N. Motta, and J. Purans, Solid State Commun. **49**, 887 (1984). The presence of the breathing-type local lattice distortion in the superconducting compositions, however, remains controversial whereas the tilting is more likely to survive [T. Egami (private communication)].

[8]H. Takagi, S. Uchida, S. Tajima, K. Kitazawa, and S. Tanaka, in *Proceedings of the International Conference on the Physics of Semiconductors, Stockholm,* edited by O. Engstrom (World Scientific, Singapore, 1986), p. 1815.

[9]L. F. Mattheiss and D. R. Hamann, Phys. Rev. B **26**, 2686 (1982).

[10]K. Takegahara and T. Kasuya, J. Phys. Soc. Jpn. **56**, 1478 (1987).

[11]A. I. Liechtenstein, I. I. Mazin, C. O. Rodriguez, O. Jepsen, and O. K. Andersen, Phys. Rev. B **44**, 5388 (1991).

[12]Z.-X. Shen, P. A. P. Lindberg, B. O. Wells, D. S. Dessau, A. Borg, I. Lindau, W. E. Spicer, W. P. Ellis, G. H. Kwei, K. C. Ott, J.-S. Kang, and J. W. Allen, Phys. Rev. B **40**, 6912 (1989).

[13]H. Matsuyama, T. Takahashi, H. Katayama-Yoshida, and Y. Okabe, Phys. Rev. B **40**, 2658 (1989).

[14]G. K. Wertheim, J. P. Remeika, and D. N. E. Buchanan, Phys. Rev. B **26**, 2120 (1982).

[15]H. Sakamoto, H. Namatame, T. Mori, K. Kitazawa, S. Tanaka, and S. Suga, J. Phys. Soc. Jpn. **56**, 365 (1987).

[16]F. M. F. de Groot, J. C. Fuggle, and J. M. van Ruitenbeek, Phys. Rev. B **44**, 5280 (1991).

[17]T. J. Wagener, H. M. Meyer III, D. M. Hill, Y. Hu, M. B. Jost, J. H. Weaver, D. G. Hinks, B. Dabrowski, and D. R. Richards, Phys. Rev. B **40**, 4532 (1989).

[18]Z. X. Shen, D. S. Dessau, B. O. Wells, C. G. Olson, D. B. Mitzi, L. Lombado, R. S. List, and A. J. Arko, Phys. Rev. B **44**, 12 098 (1991).

[19]J. J. Yeh and I. Lindau, At. Data Nucl. Data Tables **32**, 1 (1985).

[20]H. Namatame, A. Fujimori, H. Eisaki, H. Takagi, and S. Uchida, Physica C **185-189**, 2725 (1991).

[21]Effects of the O 1*s* core-hole potential on the threshold energy in O 1*s* XAS are not well understood at present. Therefore core-hole effects have been neglected in the present analysis, which may result in errors in the energy positions of unoccupied states relative to E_F, possibly by $\lesssim 1$ eV. Also, the distortion of unoccupied states caused by the O 1*s* core-hole potential will have to be considered in the analysis of detailed spectral line shapes. However, we believe that these core-hole effects are not important for the gross spectral features and the energy positions of the unoccupied states as discussed in the present paper.

[22]H. Namatame, A. Fujimori, H. Eisaki, H. Takagi, and S. Uchida, in *The Physics and Chemistry of Oxide Superconductors,* edited by Y. Iye and H. Yasuoka (Springer-Verlag, Berlin, 1992), p. 165.

[23]The uniformity of the correction to the LDA energies would be a reasonable approximation as indicated by recent theoretical studies, e.g., self-energy corrections in Si calculated using the GW approximation show rather uniform (0.58–0.68 eV) shifts of the valence- and conduction-band states compared to LDA, leading to an increase of the band gaps by ~0.6 eV [R. W. Godby, M. Schlüter, and L. J. Sham, Phys. Rev. B **37**, 10 159 (1988)].

[24]J. F. Federich, B. I. Greene, E. H. Hartford, and E. S. Hellman, Phys. Rev. B **42**, 923 (1990).

[25]W. Markowitsch, V. Schlosser, W. Lang, K. Remschnig, and P. Pogl, Physica C **185-189**, 995 (1991).
[26]H. Namatame, A. Fujimori, Y. Tokura, M. Nakamura, K. Yamaguchi, A. Misu, H. Matsubara, S. Suga, H. Eisaki, T. Ido, H. Takagi, and S. Uchida, Phys. Rev. B **41**, 7205 (1990); J. W. Allen, C. G. Olson, M. B. Maple, J. S. Kang, L. Z. Liu, J. H. Park, R. O. Anderson, W. P. Ellis, J. T. Markert, Y. Daliachaouch, and R. Liu, Phys. Rev. Lett. **64**, 595 (1990).
[27]Y. Ohta, K. Tsutsui, W. Koshibae, T. Shimozato, and S. Maekawa, Phys. Rev. B **46**, 14 022 (1992).
[28]C. Y. Chen, N. W. Preyer, P. J. Picone, M. A. Kastner, H. P. Jenssen, D. R. Gabbe, A. Cassano, and R. J. Birgeneau, Phys. Rev. Lett. **63**, 2307 (1989).
[29]R. J. Cava, P. Gammel, B. Batlogg, J. J. Krajewski, W. F. Peck, Jr., L. W. Rupp, Jr., R. Felder, and R. B. van Dover, Phys. Rev. B **42**, 4815 (1990); R. Classen, M. G. Smith, J. B. Goodenough, and J. W. Allen, *ibid.* **47**, 1788 (1993).
[30]H. Takagi, H. Eisaki and S. Uchida (unpublished).
[31]N. W. Aschcroft and N. D. Mermin, *Solid State Physics* (Saunders College, Philadelphia, 1976).
[32]T. M. Rice and L. Sneddon, Phys. Rev. Lett. **47**, 689 (1981).
[33]D. Yoshioka and H. Fukuyama, J. Phys. Soc. Jpn. **54**, 2996 (1985).
[34]J. O. Sofo, A. A. Aligia, and M. D. Nuñez Regueiro, Phys. Rev. B **40**, 6955 (1989).
[35]D. N. Manh, D. Mayou, and F. Cyrot-Lackmann, Solid State Commun. **79**, 723 (1991).
[36]Y. Inada and C. Ishii, J. Phys. Soc. Jpn. **59**, 2124 (1990).
[37]R. M. Noack, D. J. Scalapino, and R. T. Scalettar, Phys. Rev. Lett. **66**, 778 (1991).